THE JOURNAL OF PHYSICAL CHEMISTRY B

ARTICLE

pubs.acs.org/JPCB

Anhydrous Proton-Conducting Membrane Based on Poly-2-Vinylpyridinium Dihydrogenphosphate for Electrochemical Applications

Bo Yang,[†] A. Manohar,[†] G. K. Surya Prakash,[†] Weibo Chen,[‡] and S. R. Narayanan*[,†]

[†]Loker Hydrocarbon Research Institute, Department of Chemistry, University of Southern California, Los Angeles, California 90089, United States

[‡]Creare Inc., Hanover, New Hampshire 03755, United States

Supporting Information

ABSTRACT: Anhydrous electrolytes with high proton conductivity and adequate chemical stability in the temperature range of 120−180 °C can be very useful in electrochemical devices such as fuel cells, sensors, and electrolyzers. Developing such proton-conducting materials has been challenging. We have fabricated and characterized the performance of such membranes, based on poly-2-vinylpyridinium dihydrogenphosphate (P2VP-DHP), that can operate in the range of 105−180 °C under anhydrous conditions. The ionic conductivity of the membrane was 0.01 S cm^{-1} at 140 °C. Proton conduction occurs by ionization of the quaternary ammonium group and by Grotthus-type transport that involves the rapid rotation of the dihydrogenphosphate anion. The activation energy for proton transport was 50 kJ/mol. The transport number of the proton was measured by impedance spectroscopy and potential-step techniques. The measured value was in the range of 0.17−0.20. A membrane-and-electrode assembly using the P2VP-DHP was tested as an electrochemical hydrogen pump. This demonstration shows the advantage of membranes based on a polymer amine salt in electrochemical applications that require operating under water-free conditions. Weight loss measurements at 120 °C in air confirmed the thermal and oxidative stability of the membrane. The properties of the P2VP-DHP membrane reported here provide the basis for further development of proton-conducting polymer electrolyte membranes for operating temperatures above 100 °C in anhydrous environments.

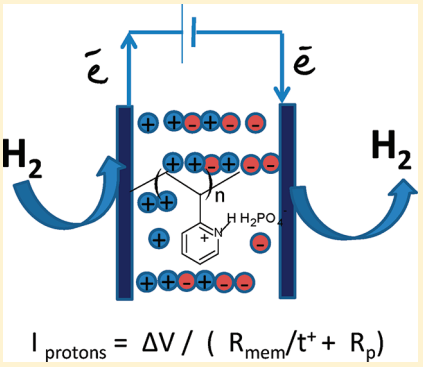

INTRODUCTION

Proton conducting membranes are used widely in electrochemical devices that include fuel cells, electrolyzers, sensors, and electrosynthetic reactors.[1] Such membranes are commonly cation exchange polymers such as Nafion wherein solvated hydronium ions are the de facto proton carriers. At temperatures higher than the boiling point of water, the conductivity of such membranes decreases dramatically because water content in these membranes decreases to a small value.[2,3] The low conductivity of such water-based membranes above 100 °C presents a severe limitation for electrochemical devices that need to operate in the temperature range of 120−200 °C. Operation in this higher temperature range provides at least three major advantages for the electrochemical devices: (1) smaller and simpler heat rejection systems, (2) higher efficiency due to improved kinetics of reactions, and (3) greater ability to tolerate catalyst poisons such as carbon monoxide in the fuel supply.

Developing a viable solid-state polymeric proton conductor with high thermal and oxidative stability and high proton conductivity in the temperature range of 120−180 °C is a major materials challenge.[4] Consequently, many different approaches have been investigated in response to this challenge. Polymeric sulfonated acid membranes and composite membranes with additives that help to retain water can provide sufficient proton conductivity at temperatures up to 120 °C and relative humidity higher than 25%.[5−11] However, these membranes cannot operate under truly anhydrous conditions. Membranes based on phosphoric acid-doped polybenzimidazole membranes conduct protons over a limited range of 160−200 °C. These membranes rely on the presence of excess phosphoric acid to facilitate proton transport.[12,13] Thus, the conductivity of these membranes can decrease due to the loss of phosphoric acid.[14] Membranes using imidazole side groups as proton carriers are promising anhydrous proton conductors. However, retaining their conductivity is still quite low for practical applications.[15] Aprotic nonaqueous liquids have also been shown to be effective as proton carriers.[16] Nonpolymeric inorganic membranes based on cesium hydrogen phosphate exhibit impressive proton conductivity at 230 °C under anhydrous conditions but are not sufficiently conductive at temperatures closer to 120 °C.[17,18]

Studies by Lassagues et al. and our group have shown that polymeric quaternary ammonium salts can conduct protons in

Received: July 15, 2011
Revised: October 18, 2011
Published: October 27, 2011

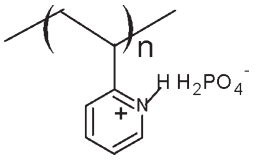

Figure 1. Poly-2-vinylpyridine dihydrogenphosphate (P2VP-DHP).

the absence of water or any other liquid-phase proton-carrier.[19,20] The proton transport in these polymer salts occurs by the ionization of the quaternary ammonium groups followed by proton transfer to the anionic groups and reorganization of the polymer backbone by flexing. The conductivity was correlated with the acid−base properties of the amine and the anion. The bisulfates and dihydrogenphosphates of poly-2-vinylpyridine (P2VP) and poly-4-vinylpyridine (P4VP) were investigated at temperatures as high as 180 °C.[19] We found that the P2VP salts were more conductive than the P4VP salts. The dihydrogenphosphates were more conductive than the bisulfates. Furthermore, polyvinylpyridinium salts are more stable than polyaromatic sulfonic acids such as polyethersulfone sulfonic acid or polystyrenesulfonic acid when subjected to thermal and oxidative stress.[21]

In this report, we focus on studying the properties of membranes based on poly-2-vinylpyridinium dihydrogenphosphate. We fabricated membrane samples and used these samples to assemble a membrane-and-electrode assembly. The ionic conductivity of the membranes was measured over the temperature range of 105−140 °C under anhydrous conditions. The transport number for the proton was determined. We also verified the proton-conducting properties of the membrane through steady-state electrochemical hydrogen pumping experiments. These studies improve our understanding of proton-conduction in polymeric amine salt based membranes and also guide the further development of anhydrous proton conductors.

EXPERIMENTAL METHODS

Preparation of Membranes and Test Cells. P2VP with an average molecular weight of 200,000 Da (Scientific Polymers Inc.) was dissolved in methanol and reacted with the stoichiometric amount of phosphoric acid under reflux in air at 80 °C for 4 h to quaternize all the pyridine moieties in the polymer. The P2VP-DHP salt (Figure 1) precipitated from the reaction mixture. The salt was washed repeatedly with methanol until it was free of excess phosphoric acid and the unreacted amine. A concentrated aqueous solution of the P2VP-DHP salt was cast on to a porous, binder-free, nonwoven polybenzoxazole mat (Zylon 25 g/m^2). This was followed by drying at 100 °C for 24 h to remove water from the membrane. The membrane was then heated in air to 120 °C for 60 h to remove any remaining water. To ensure that the membrane was water-free, the weight loss of the membrane was monitored at 120 °C. Ninety percent of the mass of the dry membrane was the polymer salt, and the support constituted the remaining 10%. The prepared membranes were sealed in plastic bags until they were assembled into electrochemical cells.

Electrochemical cells were set up with the membrane−electrode assemblies (MEA) prepared by bonding electrocatalyst-coated electrodes to either side of the P2VP-DHP membrane. A platinum catalyst (fuel cell grade; 20 m^2/g; Johnson Matthey) was combined with about 50 wt % of the polymer salt and water to form a catalyst ink. The ink was coated on Toray carbon paper (TGPH-060, 10% teflonized) and dried.

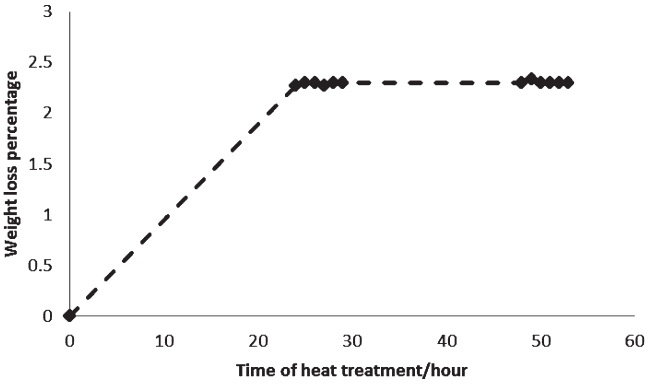

Figure 2. Membrane weight loss measurements at 120 °C in air.

The catalyst loading on each electrode was 8 mg/cm^2. The coated electrodes were bonded to the membrane (625 μm thick) under a pressure of 100 N/cm^2 at 140 °C to form an MEA with an active electrode area of 5 cm^2. The MEA was assembled in fuel cell test hardware (Electrochem Inc.). Silicone gaskets provided the sealing.

Electrochemical Testing. A schematic of the test set-up used for electrochemical studies is available as Supporting Information. The cell was pressurized up to 2 atm, and the valves on either side of the cell were left closed to check for any gas leakage. By adjusting the compression of silicone gaskets during the assembly of the cell, the leakage of hydrogen gas at 140 °C was reduced to an insignificant value. A flow of ultrahigh-purity argon was maintained through the cell for 12 h at 140 °C to remove any traces of moisture that could have been absorbed by the membrane during cell assembly. Impedance and direct-current polarization measurements were made with an impedance response analyzer/potentiostat (Princeton Applied Research PAR 2273). During impedance measurements, either ultrahigh-purity argon or hydrogen gas was allowed to flow over both the electrodes at a pressure of 1.3 atm. During the potential-step and galvanostatic hydrogen pumping experiments, only ultrahigh-purity hydrogen was used. The pressure of hydrogen on both sides of the cell was kept at 1.3 atm during the potential-step experiment. During the pumping experiments, the pressure differential across the cell was kept under 1 atm to ensure that leakage of hydrogen did not occur.

RESULTS AND DISCUSSION

Thermal Stability. Following casting and drying, the P2VP-DHP membrane was heated in air at 120 °C for 50 h. After an initial weight loss of about 2.5% in the first 24 h, no further weight loss was observed (Figure 2). The initial weight loss was attributed to the removal of residual water from the membrane-casting step. The constant weight after 24 h proved that the membrane was dry and also chemically stable in air at 120 °C. The P2VP-DHP membrane, unlike polyaromatic sulfonic acid based membranes, does not undergo rapid desulfonation and cross-linking when heated under anhydrous conditions.[16] The protonation of the nitrogen in the pyridine moiety of P2VP deactivates the aromatic ring and the side chain for oxidation. This oxidative stability has been demonstrated by pyridinium salts used as oxidizing agents in organic chemistry, such as the reagent pyridinium chlorochromate.[22] Also, cross-linking pathways that can be thermally activated are not present in the P2VP-DHP membrane.

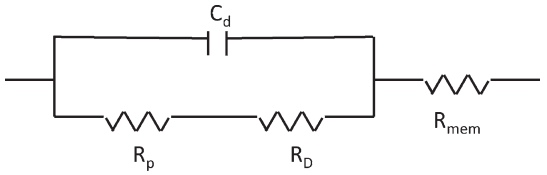

Figure 3. Electrical equivalent circuit for the membrane electrode assembly based on P2VP-DHP. R_p is the polarization resistance for the electron transfer process, C_d is the double layer capacitance, R_D is the diffusional resistance, and R_{mem} is the membrane resistance.

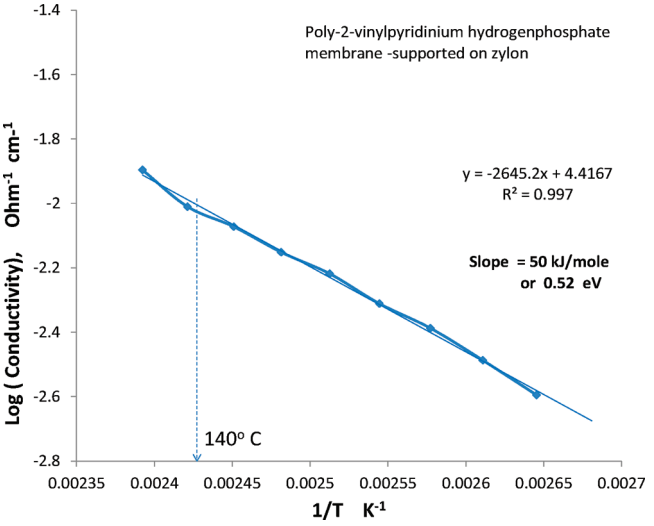

Figure 4. Ionic conductivity as a function of temperature for the P2VP-DHP membrane.

Ionic Conductivity. The ionic conductivity of the membrane was determined from impedance measurements. The cell impedance was measured at various frequencies from 100 kHz to 0.001 Hz using an ac excitation voltage of 2 mV (peak to peak). The small voltage perturbation ensured that the current−voltage response was in the linear regime. The impedance data was analyzed using the equivalent circuit shown in Figure 3.

The real component of the impedance at 100 kHz was attributed almost entirely to the resistance of the membrane, R_{mem}. The area specific resistance of the cell at this frequency was in the range of 5 to 15 Ohm cm^2. This value was substantially larger than any contributions to the resistance from the contacting hardware. The specific ionic conductivity of the membrane at 140 °C was 0.01 S cm^{-1}. The dependence of ionic conductivity on temperature followed the Arrhenius relationship, and the activation energy was 50 kJ/mol (Figure 4). On the basis of our earlier studies, we correlated the activation energy of proton transport with the free energy of dissociation for the amine salt.[19] The standard free energy change for the dissociation of pyridinium dihydrogenphosphate in the following reaction was calculated to be +23 kJ/mol.

$$\text{2-vinylpyridine-NH}^+(\text{H}_2\text{PO}_4^-) = \text{2-vinylpyridine-N} + \text{H}_3\text{PO}_4 \quad (1)$$

The observed activation energy is in the range of this free energy change but approximately twice the value. This deviation could be because we have 2-vinylpyridine as a polymer in the anhydrous form, while the calculated values were based on measurements in an aqueous medium where the ions are solvated. Further, the polymeric amine salt and the conjugate acid are quite distant from the standard state conditions assumed in the calculations.

Interfacial Processes. The impedance of the cell was measured in the presence of argon (inert gas) and hydrogen as a function of the frequency of the applied alternating voltage (Figure 6). The data was analyzed using an electrical equivalent circuit (Figure 3) for the various processes that occur at the interface. The electrical equivalent circuit represents electron transfer, charging of the double layer, diffusion of electroactive species, and migration of ions through the membrane.

As discussed earlier here, in the frequency range of 10−100 kHz, the real component of the complex impedance is associated with the migration of ions in the membrane. This impedance corresponds to R_{mem} in the equivalent circuit, and R_{mem} is used to calculate the ionic conductivity of the membrane.

The semicircular arc that appears in the frequency region of 50 Hz to 10 kHz is due to the double layer capacitance at the electrode/electrolyte interface and the electron transfer reaction

$$\text{H}^+ + \text{e}^- = \frac{1}{2}\text{H}_2 \quad (2)$$

This semicircular arc is unaffected in shape and size when the gas was switched from hydrogen to argon (Figure 5, inset). The polarization resistance R_p associated with the electron transfer process decreased with increasing temperature following the Arrhenius relationship with an activation energy of 38 kJ/mol (Figure 6). The double layer capacitance, C_d, however, did not vary significantly over the temperature range studied. Using a value of 30 μF cm^{-2} for the double layer capacitance of a flat electrode/electrolyte interface, the roughness factor was calculated to be about 2. Using the polarization resistance values at 140 °C, the value for activation energy of 38 kJ/mol, and the roughness factor, the exchange current density at 25 °C was calculated to be 1.5 × 10^{-3} A/cm^2. This value of exchange current density matches the reported values for the H^+/H_2 redox process on platinum[23] and validates the model used to analyze the impedance data in the frequency range of 50 Hz to 10 kHz.

The use of argon instead of hydrogen did not make a difference to the impedance plots in the frequency range of 50 Hz to 100 kHz (Figure 5, inset). This can be explained as follows: the electron transfer process (eq 2) can occur by the reduction of the protons in the membrane to adsorbed hydrogen. The charge transferred in this reaction during each cycle of the applied ac signal of frequency 50 Hz to 100 kHz is fairly small to be limited by the mass transfer processes. Thus, the presence of hydrogen gas does not have any significant impact on the observed impedance in this frequency range. However, at lower frequencies (<10 Hz), the charge transferred during the above reaction (eq 2) during every cycle of the applied signal becomes appreciable. Therefore, a sustained supply of protons and hydrogen becomes necessary. This results in a continuous demand for protons and hydrogen in each cycle and a reliance on the kinetics of the mass transport processes. Consequently, at frequencies below 10 Hz, the impedance with hydrogen at the electrodes was remarkably lower than that with argon at the electrodes. This observation is a direct evidence that the interface supports the electron transfer process involving protons and hydrogen.

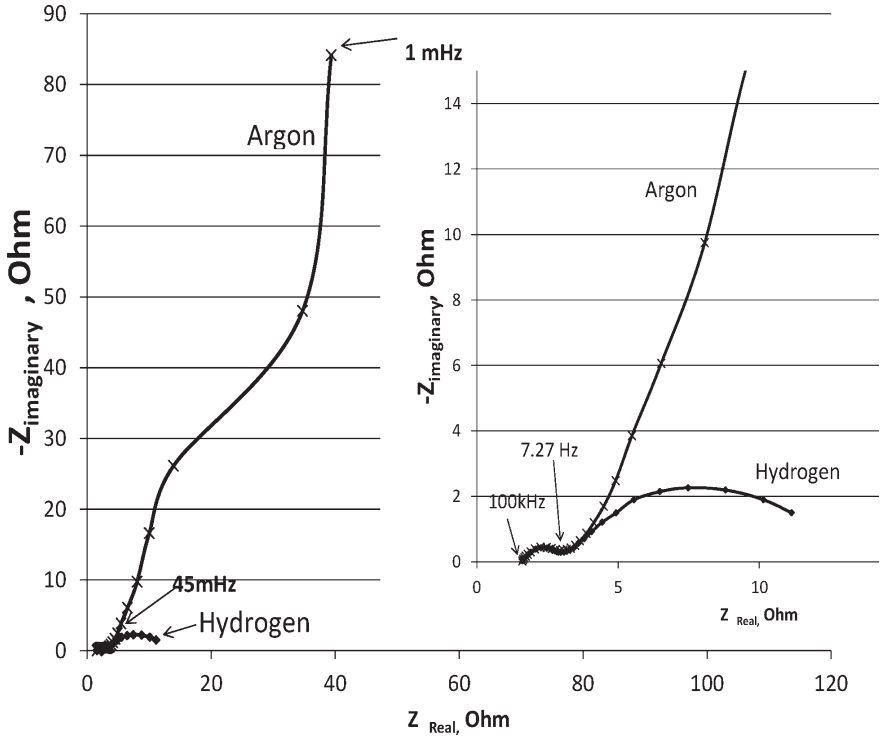

Figure 5. Impedance of P2VP-DHP membrane-electrode assemblies in argon and hydrogen.

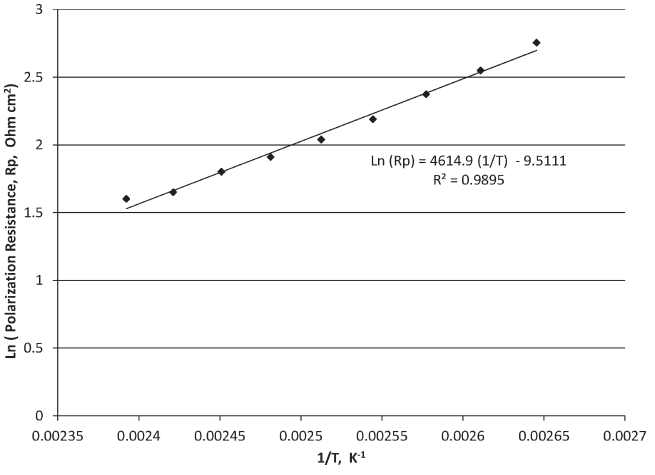

Figure 6. Variation of the polarization resistance for electron transfer with temperature.

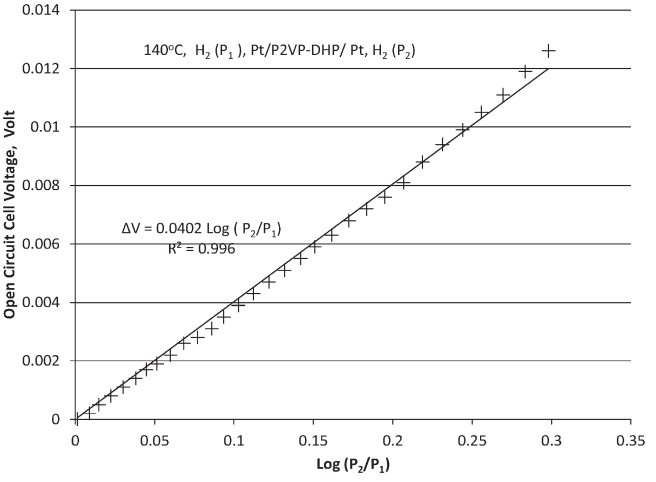

Figure 7. Open-circuit potential of cell with hydrogen pressures P_1 and P_2 on either side of the cell.

In the presence of an abundance of hydrogen gas, the semicircular arc in the impedance plot (Figure 5) in the frequency range of 1 Hz to 0.001 Hz is attributed to the mass transport of protons. These features also suggest that the diffusion and migration of protons are not entirely coupled (unlike in Nafion) and that the transport number for the proton in P2VP-DHP is less than unity (see later for discussion on transport numbers). Diffusion under semi-infinite boundary conditions is associated with a line (classical Warburg element) with a phase angle of 45 degrees on the complex−plane impedance plot. However, when diffusion distance is only a finite length, a semicircular arc is observed in the complex plane plot. For a diffusion length of δ and diffusion coefficient of D, the semicircular arc is observed at frequencies below D/δ^2.[24−26] For a diffusion coefficient of 1×10^{-5} cm^2 s^{-1} and a membrane thickness of 500 μm, the characteristic frequency for the turning over of the 45° line to the semicircular arc is 4 mHz. In the case of the P2VP-DHP membrane, we observe that the line begins to turn into a semicircular arc below 10 mHz (Figure 5). Thus, we are in the range of parameters where the finite diffusion must be considered. This is further borne out by the potential-step experiments described later.

Proton/Hydrogen Electrochemical Equilibrium. The electrochemical equilibrium of protons and hydrogen according to reaction 2 at the platinum/P2VP-DHP interface will give rise to an electrode potential, and the cell voltage will obey the Nernst

dx.doi.org/10.1021/jp206774c |J. Phys. Chem. B 2011, 115, 14462–14468

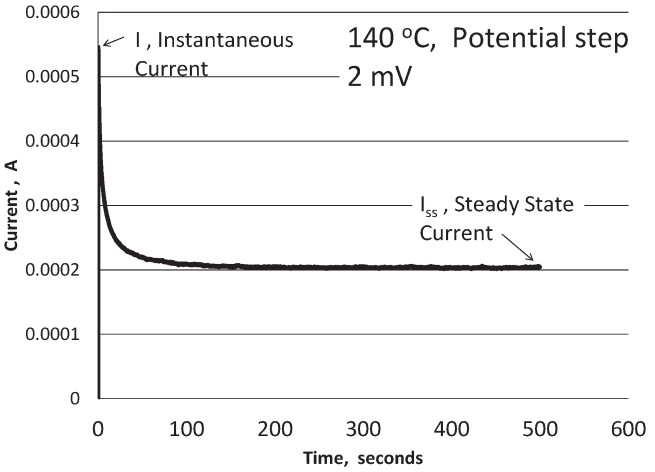

Figure 8. Transient current response to the potential-step of 2 mV.

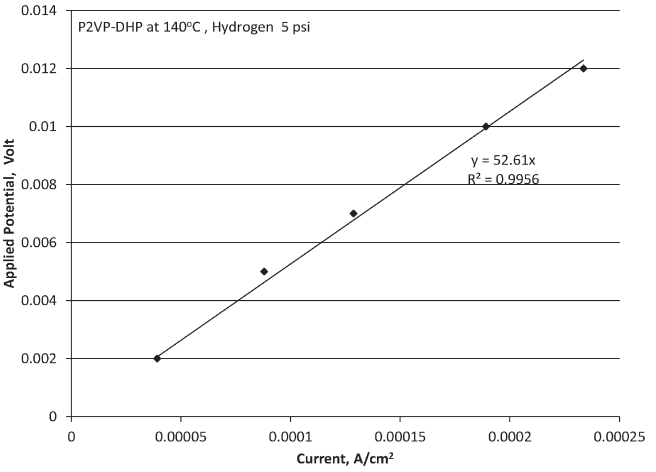

Figure 9. Dependence of steady-state current on the applied potential in the potential-step experiment.

equation. Figure 7 is the plot of the open circuit cell voltage as a function of the ratio of the pressure of hydrogen gas at the two electrodes. The slope of this curve is 0.0402 V and is in good agreement with the theoretical value of 0.0408 V for 140 °C for a Nernstian equilibrium. This agreement also confirms that a reversible proton/hydrogen equilibrium is established readily at the Pt/P2VP-DHP interface, and the analysis of the impedance data presented above is valid.

Transport Number of Proton. In the P2VP-DHP membrane, the protons and the dihydrogenphosphate ion contribute to the observed ionic conductivity. The ratio of the current transported by the protons to the total ionic current is defined as the transport number. When one kind of ion carries all the ionic current, this ion has a transport number of unity. In Nafion, the protons are the only mobile ionic species, and thus, the transport number of the proton is unity. When more than one type of ion carries the current as in an aqueous solution of sulfuric acid, the transport number of the proton is less than unity. When the transport number of an ion is unity, the movement of these ions does not cause concentration changes in the bulk of the electrolyte. However, when the charge is carried by more than one kind of ion, concentration gradients ensue. Concentration gradients of charged particles result in potential gradients that will limit the ion transport rates. Thus, the transport number is a very useful parameter that characterizes mass transport in ionic systems.

To determine the transport number, we have used the potential-step method[27] popularized by Bruce and Vincent[25,28] along with data from impedance measurements. When the cell is subjected to a potential-step with an abundance of hydrogen gas present at both the electrodes, a current that decreases with time is observed. The current transient data (Figure 8 is an example for a potential-step of 2 mV) can be used to calculate the transport number. If the transport number were unity as in the case of Nafion, no such transient in the current response will be observed.

In the potential-step experiment, as soon as the potential is imposed, current flow results from the movement of all the mobile ions (protons and dihydrogenphosphate). The current is used for double layer charging and the faradaic processes of hydrogen oxidation at the positive electrode and proton reduction at the negative electrode. To sustain this current, protons produced at the positive electrode must be transported to the negative electrode. When the transport number of the proton is less than unity, other ions will also participate in the conduction process, resulting in the accumulation of protons at the positive electrode and depletion of protons at the negative electrode. These concentration changes in turn cause the equilibrium electrode potential to change in a direction that opposes the flow of current, resulting in a decrease in the observed current. The concentration changes at the two electrodes also set up a net diffusional flux of protons from the positive to the negative electrode, and this flux increases with time. When the diffusion flux of protons becomes equal to the rate of faradaic reaction, a steady-state is reached, and the current does not decrease any more. Thus, the current transient observed is the approach to a steady-state concentration distribution of ions following the perturbation by the potential-step.

The electrical equivalent circuit used for impedance analysis (Figure 3) was also applied to the analysis of transient data to calculate the transport number. The steady-state current I_{ss} for a potential-step of ΔV is given by the following equation:

$$I_{SS} = \frac{\Delta V}{(R_{mem}/t^+) + R_p} \quad (3)$$

By rearranging eq 3, the transport number t^+ is given by

$$t^+ = \frac{I_{SS}R_{mem}}{(\Delta V - I_{SS}R_p)} \quad (4)$$

where R_p is the polarization resistance for the electron transfer process. The diffusion impedance for proton transport, R_D in the equivalent circuit, is related to the membrane resistance R_{mem} through the transport number as $R_{mem}\ (1/t^+ - 1)$; this satisfies the condition that R_D would be zero when the transport number t^+ is unity.

Some authors make the approximation that the polarization resistance R_p is small relative to the membrane resistance R_{mem}. However, the impedance data (Figure 5) suggest that the values of R_{mem} and R_p are comparable, and such an approximation is not valid in the present case. R_p is calculated by curve-fitting to the semicircular portion of the impedance data in the frequency region of 50 kHz to 5 Hz. R_{mem} is determined from the real component of the impedance at high frequency, as in the ionic conductivity measurements. Also, the steady-state current I_{ss} is

related to the potential-step ΔV by

$$\Delta V = I_{SS}(R_p + R_D + R_{mem}) \quad (5)$$

The slope of the plot of ΔV vs I_{ss} (Figure 9) was used to calculate R_D using values of R_{mem} and R_p obtained from impedance analysis.

Using the values of R_p = 5.2 Ohm cm^2, R_{mem} = 8.0 Ohm cm^2, and R_D =38.2 Ohm cm^2, the transport number according to eq 4 for various values of ΔV in the range of 2 mV to 12 mV was 0.17 to 0.18. This value is also in close agreement with the ratio of $R_{mem}/(R_D + R_{mem})$ of 0.2. Thus, various methods of calculating the transport number gave very similar values. The transport number can also be calculated from the transient data using the instantaneous value of current I as per the following equation:

$$t^+ = \frac{I_{SS}\Delta V}{I(\Delta V - I_{SS}R_p)} \quad (6)$$

A calculation based on eq 6 is also expected to yield the same results.[25,26] However, this approach requires an accurate determination of the instantaneous current. We found that the measurement of the instantaneous current I at $t = 0^+$ was prone to error depending on the instrument capabilities and the sampling rate chosen. No such limitation was found with estimating I_{ss}. Therefore, we recommend the use of impedance data with the steady-state current values from the potential-step experiment to calculate the transport number.

The relatively low value of the transport number could be because of the multiple barriers for proton transport as evidenced in the high activation energy for ionic conductivity. For the protons to conduct, they must first dissociate from the cations and bond to the dihydrogenphosphate anion. This must be followed by the rotation of the dihydrogenphosphate and delivery of the proton to a deprotonated site in the vicinity. The probability and frequency of these events affect the concentration of proton charge carriers and also their mobility. However, the migration of the dihydrogenphosphate ion can occur readily in an electric field by a straightforward process of translation with assistance from the flexing of the membrane chains and without a bond-breaking event. Therefore, we can expect a higher transport number for the dihydrogenphosphate ion than for the proton.

With a proton transport number of 0.2, the proton conductivity of the membrane at 140 °C is lower than the ionic conductivity, a distinction that is not often drawn in the literature. The proton conductivity is calculated to be 2×10^{-3} S cm^{-1}. Since the membrane is loaded only to the extent of 90% with the polymer, the proton conductivity of the P2VP-DHP salt is 2.2×10^{-3} S cm^{-1}.

Electrochemical Pumping of Hydrogen. Hydrogen at low pressures can be pumped up to higher pressures using an electric current in an electrochemical cell.[29] During the passage of current through the cell, the oxidation of hydrogen to protons occurs at the positive electrode and protons are reduced to hydrogen at the negative electrode. If the hydrogen produced at the negative electrode is allowed to accumulate, the pressure of the hydrogen will rise above the value at the positive electrode. This process is referred to as hydrogen pumping. Such electrochemical pumping is the most direct proof of the proton transport properties of the membrane.

When membranes such as Nafion are used for electrochemical pumping, water is supplied to the positive electrode, since water is transported across the membrane by electro-osmotic drag to the negative electrode. Thus, hydrogen generated at the negative electrode is also rich in water.[30]

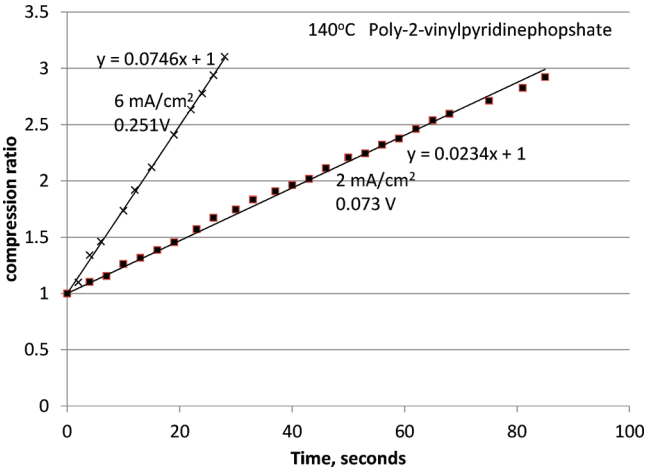

Figure 10. Compression of hydrogen at 140 °C using the P2VP-DHP membrane.

Using the P2VP-DHP membrane in the anhydrous state as a proton conductor, we were able to demonstrate the electrochemical pumping of dry hydrogen. With the passage of current, the pressure of hydrogen on the negative electrode side was increased to 1.5 times the pressure on the positive electrode (Figure 10). The linear increase in pressure with current density shows that there is no leakage of hydrogen from the cell or across the membrane. Also, the rate of hydrogen compression (as indicated by the slope of lines in Figure 10) is proportional to the current as is expected from Faraday's laws of electrolysis. The experimental hardware was limited to the maximum pressure of 2.5 atm. However, with additional support for the membrane and improved sealing, higher pressures can be attained.

The hydrogen pumping experiment shows how anhydrous membranes can be used to pump water-free hydrogen. This type of hydrogen pumping can also be used to purify hydrogen gas streams as demonstrated recently with a phosphoric acid-doped polybenzimidazole membrane.[31]

The efficiency of the hydrogen compression process is defined as the ratio of the theoretical energy to the actual energy consumed. At 140 °C and a compression ratio of 1.5, the theoretical cell voltage is 0.0072 V. In practice, we had a steady-state voltage of 0.073 V at 2 mA/cm^2. The compression efficiency is calculated to be about 10%. Ninety-five percent of the efficiency loss results from the resistance of the membrane. By using a membrane that is just 200 μm thick, the efficiency can be increased to about 30%.

CONCLUSIONS

Water-free proton conducting membranes have been fabricated with poly-2-vinylpyridinium dihydrogenphosphate. The membranes are thermally and oxidatively stable in air at 105−140 °C, and their ionic conductivity is in the range of 0.01 S cm^{-1}. The ionic conductivity increases with temperature in accordance with Arrhenius law, and the activation energy for ionic conduction was 50 kJ/mol. This value of activation energy matches the free energy change for the dissociation of the pyridinium salt. We have identified the various interfacial

processes that occur in the membrane electrode assembly. The reversible redox process involving hydrogen and protons is shown to readily occur at the membrane−electrode interface. The transport number of the proton was in the range of 0.17−0.20. We have determined the transport number of the proton by a method that combines the advantages of impedance spectroscopy and potential-step techniques. The proton transport properties of the membrane have also been demonstrated by electrochemically pumping dry hydrogen. This experiment also shows the potential applications of these membranes in electrochemical devices such as hydrogen compressors, electrolyzers, and fuel cells.

■ ASSOCIATED CONTENT

Supporting Information. Details of the experimental set-up used. This material is available free of charge via the Internet at http://pubs.acs.org.

■ AUTHOR INFORMATION

Corresponding Author
*E-mail: sri.narayan@usc.edu.

■ ACKNOWLEDGMENT

The research reported here was funded by an STTR program from the Missile Defense Agency and was also partly supported by the Loker Hydrocarbon Research Institute, University of Southern California, Los Angeles. We acknowledge Dr. Robert Aniszfeld for his support during the course of these studies and H. Yoshioka of Ni Teijinshoji (USA) Ltd. for the supply of the Zylon material.

■ REFERENCES

(1) Vielstich, W. A., Lamm, A., Gasteiger, H. A., Eds. *Handbook of Fuel Cells: Fundamentals, Technology, Applications*; John Wiley and Sons: New York, 2003.
(2) Anantaraman, A. V.; Gardner, C. L. *J. Electroanal. Chem.* **1996**, *414*, 115–120.
(3) Sone, Y.; Ekdunge, P.; Simonsson, D. *J. Electrochem. Soc.* **1996**, *143*, 1254–1259.
(4) Garland, N.; Kopascz, J. P. *J. Power Sources* **2007**, *172*, 94–99.
(5) Yang, C.; Srinivasan, S.; Bocarsly, A. B.; Tulyani, S.; Benziger, J. B. *J. Membr. Sci.* **2004**, *237*, 145–161.
(6) Shao, Y.; Yin, G.; Wang, Z.; Gao, Y. *J. Power Sources* **2007**, *167*, 235–242.
(7) Myers, D.; Niyogi, S., Proceedings of Hydrogen Fuel Cells and Infrastructure Technologies Program Review, 2006. U.S. Department of Energy. http://www.hydrogen.energy.gov/pdfs/review06/fc_1_myers.pdf.
(8) Yang, B.; Manthiram, A. *J. Electrochem. Soc.* **2004**, *151*, A2120–A2125.
(9) Ramani, V.; Kunz, H. R.; Fenton, J. M. *J. Membr. Sci.* **2004**, *232*, 31–44.
(10) Chalkova, E.; Fedkin, M. V.; Komarneni, S.; Lvov, S. N. *J. Electrochem. Soc.* **2007**, *154*, B288–B295.
(11) Kim, Y. S.; Wang, F.; Hickner, M.; Zawodzinski, T. A.; McGrath, J. E. *J. Membr. Sci.* **2003**, *212*, 263–282.
(12) Wainright, J. S.; Wang, J.-T.; Weng, D.; Savinell, R. F.; Litt, M. H. *J. Electrochem. Soc.* **1995**, *142*, L121–123.
(13) Guo, Q.; Pintauro, P. N.; Tang, H.; O'Connor, S. *J. Membr. Sci.* **1999**, *154*, 175–181.
(14) Yu, S.; Xiao, L.; Benicewicz, B. C. *Fuel Cells* **2008**, *8*, 165–174.
(15) Scharfenberger, G.; Meyer, W. H.; Wegner, G.; Schuster, M.; Kreuer, K. D. *Fuel Cells* **2006**, *6*, 237–250.
(16) Subbaraman, R.; Ghassemi, H.; Zawodzinski, T. *Solid State Ionics* **2009**, *180*, 1143–1150.
(17) Uda, T.; Haile, S. M. *Electrochem. Solid-State Lett.* **2005**, *8*, A245–A246.
(18) Taninouchi, Y. K.; Uda, T.; Awakura, Y.; Ikeda, A.; Haile, S. M. *J. Mat. Chem.* **2007**, *17*, 3182–3189.
(19) Narayanan, S. R.; Yen, S.-P.; Liu, L.; Greenbaum, S. G. *J. Phys. Chem. B* **2006**, *110*, 3942–3948.
(20) (a) Lassegues, J. C. In *Protonic Conductors*; Colomban, P., Ed.; Cambridge University Press: Cambridge, U.K., 1992; p 311. (b) Trinquet, O. Solid State Proton Conductors. Ph.D. Thesis, University of Bordeaux, 1990.
(21) Suleiman, D.; Elabd, Y. A.; Napadensky, E.; Sloan, J. M.; Crawford, D. M. *Thermochim. Acta* **2005**, *430*, 149–154.
(22) Corey, E. J.; Suggs, W. *Tetrahedron Lett.* **1975**, *16*, 2647–2650.
(23) Bockris, J. O'M. In *Modern Aspects of Electrochemistry*; Bockris, J. O'M., Conway, B. C., Eds.; Academic Press Inc.: London, 1954; Vol. 1, p 199.
(24) Boillot, M.; Didierjean, S.; Lapicque, F. *J. Appl. Electrochem.* **2004**, *34*, 1191–1197.
(25) Evans, J.; Vincent, C.; Bruce, P. *Polymer* **1987**, *28*, 2324–2328.
(26) Sorensen, P. R.; Jacobsen, T. *Electrochim. Acta* **1982**, *27*, 1671–1675.
(27) Watanabe, M.; Rikukawa, M.; Sanui, K.; Ogata, N. *J. Appl. Phys.* **1985**, *58*, 736–741.
(28) Bruce, P.; Evans, J.; Vincent, C. *Solid State Ionics* **1988**, *28−30*, 918–922.
(29) Sedlak, J. M.; Austin, L. F.; LaConti, A. B. *Int. J. Hydrogen Energy* **1981**, *6*, 45–51.
(30) Strobel, R.; Oszcipok, M.; Fasil, M.; Rohland, B.; Jorissen, L.; Garche, J. *J. Power Sources* **2002**, *105*, 208–215.
(31) Perry, K. A.; Eisman, G. A.; Benicewicz, B. C. *J. Power Sources* **2008**, *177*, 478–484.